White-Matter Connectivity between Face-Responsive Regions in the Human Brain

Markus Gschwind[1,2], Gilles Pourtois[3], Sophie Schwartz[1,2], Dimitri Van De Ville[4,5] and Patrik Vuilleumier[1,2]

[1]Laboratory for Behavioral Neurology and Imaging of Cognition, Department of Neuroscience, Faculty of Medicine, University of Geneva, CH-1211 Geneva, Switzerland, [2]Department of Neurology, University Hospital of Geneva, CH-1211 Geneva, Switzerland, [3]Department of Experimental Clinical and Health Psychology, B-9000 Ghent University, Ghent, Belgium, [4]Department of Radiology and Medical Informatics, University of Geneva, CH-1211 Geneva, Switzerland and [5]Medical Image Processing Lab, Interfaculty Institute of Bioengineering, Ecole Polytechnique Féderale de Lausanne, CH-1015 Lausanne, Switzerland

Address correspondence to Markus Gschwind, Laboratory for Behavioral Neurology and Imaging of Cognition, Department of Neurosciences, University Medical Center (CMU), 1 Michel-Servet, CH-1211 Geneva. Email: markus.gschwind@gmail.com

Face recognition is of major social importance and involves highly selective brain regions thought to be organized in a distributed functional network. However, the exact architecture of interconnections between these regions remains unknown. We used functional magnetic resonance imaging to identify face-responsive regions in 22 participants and then employed diffusion tensor imaging with probabilistic tractography to establish the white-matter pathways between these functionally defined regions. We identified strong white-matter connections between the occipital face area (OFA) and fusiform face area (FFA), with a significant right-hemisphere predominance. We found no evidence for direct anatomical connections between FFA and superior temporal sulcus (STS) or between OFA and STS, contrary to predictions based on current cognitive models. Instead, our findings point to segregated processing along a ventral extrastriate visual pathway to OFA-FFA and another more dorsal system connected to STS and frontoparietal areas. In addition, early occipital areas were found to have direct connections to the amygdala, which might underlie a rapid recruitment of limbic brain areas by visual inputs bypassing more elaborate extrastriate cortical processing. These results unveil the structural neural architecture of the human face recognition system and provide new insights on how distributed face-responsive areas may work together.

Keywords: DTI, face network, face processing, fMRI, tractography, white-matter connectivity

Introduction

Brain research has revealed a set of cortical regions specialized for face processing (Gobbini and Haxby 2007), but the exact structural organization of this network remains unknown. Following neuropsychological studies showing selective deficits in face recognition after (typically right) occipitotemporal lesions (Grüsser and Landis 1991), positron emission tomography and functional magnetic resonance imaging (fMRI) studies in healthy subjects pinpointed face-specific activation in extrastriate visual cortex, including the "fusiform face area" located on the ventral temporal lobe (FFA; Sergent et al. 1992; Kanwisher et al. 1997) and the "occipital face area" located on the lateral inferior occipital lobe (OFA; Gauthier et al. 2000). These 2 regions as well as the superior temporal sulcus (STS) are consistently found to respond to faces more than to other visual object categories (Pourtois et al. 2005a, 2009) and are generally considered to constitute a "core system" for face processing (Haxby et al. 2000). Although their exact role is still debated, FFA and OFA are thought to be critically involved in processing invariant aspects of face information that convey identity cues as well as other basic features related to race, gender, and age (Haxby et al. 2000; Rossion et al. 2003), with FFA being particularly sensitive to facial configuration and personal identity but OFA more sensitive to elementary visual features and parts (Rotshtein et al. 2005; Liu et al. 2010; Righart et al. 2010). On the other hand, STS is involved in the processing of changeable and dynamic aspects of faces, such as eye and mouth movements, as well as facial expression (Hoffman and Haxby 2000). Other brain regions also show distinctive responses to faces, including the amygdala, anterior temporal cortex, posterior cingulate, and prefrontal areas, which together constitute an "extended system" for social and affective processes (Haxby et al. 2000; Gobbini and Haxby 2007).

However, previous lesion and neuroimaging data can only indirectly infer how these cortical regions are anatomically interconnected and functionally organized. Because damage to FFA or OFA does not always impair face recognition, a critical role for some disruption of their interconnections has also been postulated (Liu et al. 2002; Sorger et al. 2007; Fox et al. 2008). Yet, the existence of direct connections between face-responsive areas has not been demonstrated. Only one fMRI study (Fairhall and Ishai 2007) investigated the functional connectivity of regions within the core and extended face recognition systems, using dynamic causal modeling (DCM). Results suggested that the core regions might be hierarchically organized in a feed-forward fashion, with the OFA sending inputs to both FFA and STS and FFA selectively projecting to limbic and prefrontal regions of the extended system (Haxby et al. 2000; Gobbini and Haxby 2007). These connectivity results reflect the temporal correlation profile between activations of the different regions, but the structural connections responsible for these functional patterns remain unresolved. Furthermore, functionally defined regions such as the FFA, OFA, and STS cannot easily be delineated in postmortem brains, and data from primate models (Tsao et al. 2008) are not directly transferable to human brain anatomy.

Diffusion tensor imaging (DTI) provides a valuable non-invasive method to delineate the anatomical connectivity between brain regions (Pierpaoli et al. 1996). The structure of different fiber pathways has been successfully dissected with DTI (Catani et al. 2003; Dougherty et al. 2005; Kim et al. 2006). However, no study has investigated the anatomical connectivity between extrastriate visual areas involved in face processing. Although DTI tractography cannot achieve the precision of postmortem tracing, it is a powerful tool to compare the pattern of connections between brain areas in vivo, showing good agreement with postmortem dissection (Stieltjes et al. 2001) and tracer studies in nonhuman primates (Dauguet et al. 2007).

Here, we combine fMRI with an established probabilistic tractography technique (Behrens et al. 2003, 2007) to characterize the white-matter connectivity between face-responsive regions (Gobbini and Haxby 2007). We analyze the connectivity pattern of each region in the "core" face-responsive system (OFA, FFA, STS), together with other key regions of the "extended" system such as the amygdala (AMG) and posterior cingulate cortex (PCC), plus a "control" region in occipital cortex (primary visual area). In addition, connections from the amygdala are of particular interest given that this structure has been shown to interact with both early (occipital) and late (temporal) stages along the ventral visual processing stream (Amaral et al. 2003; Vuilleumier 2005) and was also proposed to receive inputs from STS (Haxby et al. 2000; Calder et al. 2007). Furthermore, given the hemispheric asymmetry in face processing established by various behavioral and physiological measures (Grüsser and Landis 1991; Kanwisher et al. 1997; Rossion et al. 2003; Fox et al. 2008), we perform separate analyses for all regions in each hemisphere. Our results provide new constraints for face recognition models, by revealing for the first time the structural architecture of neural pathways in the human face recognition network and their relative asymmetry between the 2 hemispheres.

Materials and Methods

Participants
Twenty-four healthy volunteers (14 females mean age 28 years, range 19–37, all right handed) gave informed consent to participate to the study, which was approved by the local ethic committee. All had normal or corrected to normal vision and no past neurological or psychiatric history. Data of 2 participants were discarded due to technical problems in the DTI sequence, resulting in a total of 22 participants for all subsequent analyses.

Stimuli and Procedure
A standard block design was used to map the face-sensitive regions in individual participants (Kanwisher et al. 1997; Grill-Spector et al. 2004; Spiridon et al. 2006), with 16 alternating blocks of faces, places, and scrambled images (4 blocks per stimulus category, 16 stimuli in each block, 32 photographs in each category). The faces pictures showed neutral and friendly male and female faces in frontal view. The pictures of places included front view of buildings as well as landscapes without living beings. Scrambled images were created by rearranging fragments of the face and place pictures so as to prevent recognition of any meaningful stimulus (see Fig. 1). Each stimulus was presented for 750 ms with an intertrial interval of 500 ms. Participants performed a one-back detection task by pressing a button for any immediate repetition (one per block). Mean correct detection rate was 95.5%, and none of the 6 pairwise comparisons between stimulus categories was significant.

MRI Scanning
MRI images were acquired on a 3-T Trio TIM system (Siemens, Erlangen, Germany) with an 8-channel head-coil using parallel imaging (GRAPPA). Diffusion-weighted data were acquired in 2 data sets, with the following parameters: time repetition (TR)/time echo (TE)/flip angle 8200 ms/82 ms/90°, image resolution 128 × 128 with 65 slices and voxel size of 2 × 2 × 2 mm. Monopolar diffusion weighting was performed along 30 independent directions, with a b-value of 1000 s/mm². A reference image with no diffusion weighting ($b = 0$) was also obtained for each data set. For the functional localizer paradigm, whole-brain images were acquired with a gradient-echo echo-planar imaging sequence using the following parameters: TR/TE/flip angle = 2200 ms/30 ms/85°, field of view (FOV) = 211 mm, matrix = 64 × 64. Each of the total 165 functional images comprised 36 axial slices (thickness 3.4

mm; no gap) oriented parallel to the inferior edge of the occipital and temporal lobes. Additionally, for each participant, a structural image was acquired with a T_1-magnetization prepared rapid gradient echo (160 contiguous sagittal slices, FOV = 256 mm, TR/TE/flip angle = 1900 ms/2.23 ms/9°, matrix = 256 × 256, slice thickness = 0.9 mm).

Image Processing and Data Analysis

Diffusion-Weighted Data
Diffusion-weighted data were processed using the tools implemented in FSL (Version 4.1.2; www.fmrib.ox.ac.uk/fsl). The 2 raw data sets were first corrected for Eddy current distortions and motion artifacts using the correction tool (FDT 1.0) and then averaged to improve signal-to-noise ratio (Eickhoff et al. 2010) and, subsequently, skull-stripped (using BET). The principal diffusion direction was estimated for each voxel as a probability density function, using Bayes' rules in order to account for noise and uncertainty in the measured data. As described elsewhere (Behrens et al. 2003), the implicit modeling of noise in a probabilistic model enables a fiber-tracking procedure without externally added constraints such as fractional anisotropy (FA) threshold or fiber angle. Thus, fiber tracking in or near cortical areas becomes more sensitive. The use of a 2-fiber model (Behrens et al. 2007) also improved the modeling of crossing fibers. By sending out 25 000 streamline samples per seed voxel, we mapped the probabilistic connectivity distributions for each voxel in the region of interest (ROI). For each individual, the FA images were normalized into Montreal Neurological Institute (MNI) space by using a nonlinear transformation onto the FMRIB58 FA template (FNIRT, as used for the first steps of the tract-based spatial statistics [TBSS] algorithm [Smith et al. 2006]).

fMRI Data
Functional images were analyzed with the general linear model (Friston et al. 1998) for block designs, using SPM5 software (www.fil.ion.ucl.ac.uk/spm). All images were unwarped, corrected for slice timing, segmentation-based normalized to MNI space (Ashburner and Friston 2005), spatially smoothed (full-width at half-maximum 8 mm Gaussian kernel), and high-pass filtered (cutoff 1/120 Hz). Statistical analyses were performed on a voxelwise basis across the whole brain. Blocks with faces, blocks with places (houses and landscapes), and blocks with scrambled images were modeled by a boxcar function with 2 epoch types, convolved with the standard hemodynamic response function and resulting in 3 conditions: Faces, Places, and Scrambled. Movement parameters derived from the realignment procedure (3 translations, 3 rotations) were included as nuisance covariates. Parameter estimates for this general linear model were then generated at each voxel of every participant. Statistical parametric maps were computed for linear contrasts between the parameter estimates of the different conditions. We then performed random-effect group analyses on the contrast images using one sample t-tests (Friston et al. 1998).

Selection of ROIs
The face-responsive regions were delineated in each individual (in MNI space) using the peak voxel of the activation clusters identified by the contrast "faces > places + scrambled," in the functional face localizer (a well-established procedure similar to previous studies of face processing, see, e.g., (Kanwisher et al. 1997; Haxby et al. 2000; Pourtois et al. 2010a). These regions included: the FFA, OFA, posterior STS, and precuneus/posterior cingulate cortex (PCC), as well as the amygdala (AMG), orbitofrontal cortex (OFC), and inferior frontal cortex (Gobbini and Haxby 2007). For our subsequent DTI analysis, we selected the face processing core regions including FFA, OFA, and STS in each hemisphere plus PCC which is thought to be involved in face memory (Gobbini and Haxby 2007; Vrticka et al. 2009). Because the latter region was close to the midline and often merged in one single cluster including both hemispheres, it was split into 2 different activation clusters, one in the left ($x - 6$) and one in the right ($x + 6$) hemisphere. In a few cases where there was no clear-cut activation for one of these core regions (even at a level of $P < 0.05$ uncorrected), the coordinates of the group results were taken instead (this was necessary for left STS

functional face localizer scan
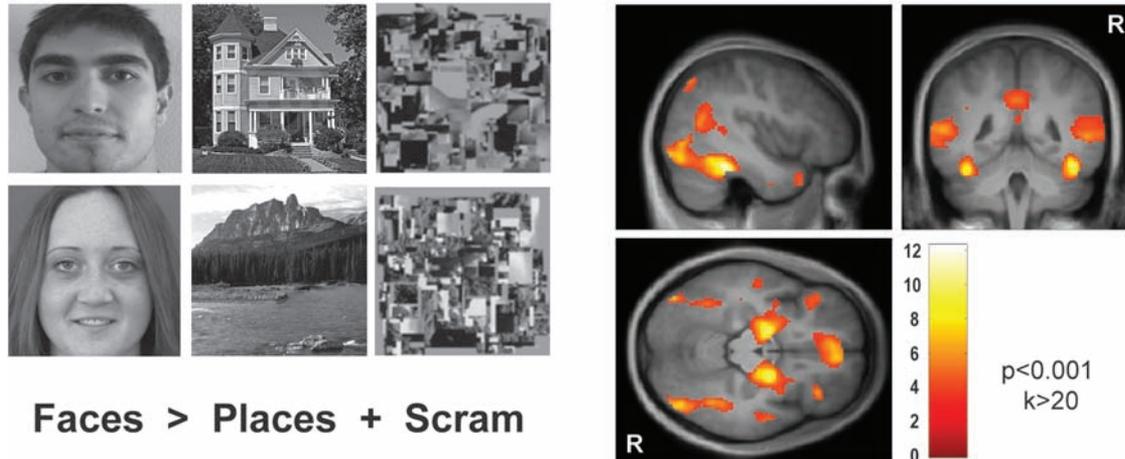
Faces > Places + Scram

Figure 1. Face network defined by fMRI. Face-selective regions were identified functionally in each individual by employing a fMRI localizer scan in a block design with 3 conditions: faces, places, and scrambled images. Group results are illustrated here, demonstrating face-selective activations (as identified by the contrast [faces > places + scrambled]) in a distributed network including occipital face area (OFA), fusiform face area (FFA), posterior superior temporal sulcus (STS), amygdala (AMG), posterior cingulate cortex (PCC), and medial OFC and inferior frontal gyrus, in both hemispheres (one sample t-test at the second RFX level, $P < 0.001$ uncorrected, $k > 20$).

in 5, right STS in 3, and PCC in 4 of 22 participants). In these cases, the peak voxel of the group cluster was extracted and retransferred back into the individual's native space, using the inverse normalization matrix (output from segmentation-based normalization of SPM5 [Ashburner and Friston 2005]). In addition, we also defined ROIs in the early visual cortex (CAL) by selecting the most occipital cluster peak in both hemispheres as obtained in an F-test across faces, places, and scrambled. Finally, the amygdalae (AMG) were determined manually on the anatomical T_1 image in each participant, in order to get the most precise and reproducible localization of these relatively small regions. Note, however, that strong bilateral amygdala activations were found in the faces > places + scrambled contrast (see Fig. 1) and that a functional definition of this ROI using the face localizer data yielded qualitatively similar results but appeared more variable due to the high variance of fMRI clusters and spatial distortions of echo planar images in these brain regions. Obviously, such anatomical localization was not possible for OFA and FFA since the latter can only be functionally defined.

All fiber-tracking analysis were conducted in the individual native DTI space. In order to bring the selected fMRI-cluster's peak voxel into the individual DTI space, a 3D rigid-body transformation was used by registering the participant's mean functional image (native space) to the diffusion $b = 0$ image, and the AMG coordinates were transferred form the individual T_1 space into the individual DTI space using the inverse transformation obtained from a rigid-body registration of the individual FA image to the individual T_1 image (FSL-FLIRT). The average MNI coordinates (and range) of each of the ROIs are listed in Table 1.

All ROIs were subsequently projected onto the white matter by dilating a sphere centered around the peak voxel, until it comprised at least 30 voxels with an FA value > 0.2, in order to allow for reliable tractography (Catani et al. 2002; Hagmann et al. 2006). The resulting volume (5.54 mm mean radius of dilatation kernel, standard deviation [SD] 0.9 mm, no hemispheric differences in paired t-tests) was used to select voxels in the white matter that served as seeds and targets for the subsequent probabilistic fiber tracking. This procedure ensured a balanced estimation of the number of connections from each seed when comparing the different ROIs (Hagmann et al. 2006).

Determination of the Major White-Matter Bundles

To analyze the relation between face-responsive ROIs and major white-matter bundles connecting posterior to anterior brain areas (see below, analysis 3), we defined 2 main white-matter fasciculi in each individual by means of fiber tracking with seeds placed in subcortical regions over the trajectory of these fasciculi (Schmahmann and Pandya 2006). The

Table 1

Face-responsive ROIs

ROI	MNI coordinates					
	x	y	z	x-range	y-range	z-range
FFA	40	−47	−21	34–48	−64 to −36	−26 to −12
	−38	−51	−20	−44 to −34	−66 to −38	−28 to −14
OFA	40	−78	−12	30–50	−94 to −68	−18 to −4
	−41	−79	−10	−52 to −34	−90 to −62	−18 to −2
STS	58	−49	10	48–68	−64 to −36	2–20
	−56	−50	12	−66 to −42	−62 to −26	4–26
PCC	4	−57	33	0–12	−68 to −50	22–44
	−6	−51	33	−12 to −2	−58 to −46	22–42
CAL	16	−95	6	10–26	−98 to −88	−4 to 16
	−14	−99	5	−24 to −6	−104 to −94	−8 to 14
AMG	26	−5	−22	19–31	−9 to −1	−29 to −20
	−25	−6	−24	−28 to −21	−10 to -0	−28 to −21

Note: Mean and range of the cluster peaks for each of the face-responsive ROI identified in the functional face localizer scan (see Fig. 1) for each participant separately (contrast face > places + scrambled images).

inferior longitudinal fasciculus (ILF) runs in long fibers through the temporal lobe, connecting the occipital pole with the temporal pole. It includes fibers arising in the superior, middle, and inferior temporal and fusiform gyri and projecting to the lingual gyrus, cuneus, lateral occipital cortex, and occipital pole (Catani et al. 2002). Although this has not been explored specifically in the past, the ILF is well situated to potentially play an important role between the face-responsive regions. The arcuate fasciculus (AF) is another major fiber bundle that was also examined, as it connects the prefrontal cortex with more posterior parietooccipital and parietotemporal regions (Catani et al. 2002).

Both the ILF and AF were identified in each hemisphere for each participant using standard approaches (Wakana et al. 2007). The ILF was determined by a 2 ROI procedure: one ROI was drawn on a coronal image slice at half distance between the occipital pole and the posterior edge of the corpus callosum over the whole hemisphere and the second ROI was drawn on a coronal slice covering the whole temporal lobe in its anterior part (Catani et al. 2003; Catani and Thiebaut de Schotten 2008). The AF was also determined using a two ROI procedure: one placed on a coronal slice through the superior longitudinal fasciculus II (SLF II; Makris et al. 2005) and one placed on the axial slice through the vertical part of the AF (Catani and Mesulam 2008; Catani and Thiebaut de Schotten 2008; Rilling et al. 2008).

Estimation of Connectivity

The connectivity analysis used to investigate the face-responsive network consisted of 3 independent and complementary analyses: "analysis 1," unrestricted connectivity maps determined for each ROI in both hemispheres; "analysis 2," pairwise connectivity values from each ROI to each other ROI within each hemisphere; "analysis 3," relation between each ROI and the 2 major white-matter bundles that are closely associated with temporo-occipital areas, that is, ILF and AF. The latter analysis allowed us to determine whether each face-responsive ROI has trajectories that merge with and presumably pass through these white-matter bundles to project to distant regions (for similar procedure, see Croxson et al. [2005]). By combining these 3 approaches, we could obtain a detailed and comprehensive picture of the structural connectivity pattern between the face-responsive ROIs.

Probabilistic fiber tracking (using FDT 1.0; see Behrens et al. [2007]) was initiated from every voxel within the binarized ROI sphere. Streamline samples (25 000) were sent out from each voxel, with a step length of 0.5 mm and a curvature threshold of 0.2. Note that for analysis 1, no restriction was used in order to explore to all brain regions to which the white-matter pathways were directed. This also served as a control to ensure that fiber tracking was indeed possible and selective. By contrast, "waypoint" and "termination" masks were applied in analysis 2 and analysis 3 in order to define the only and exact connections between a given seed and a given target. In the latter case, fiber tracking was initiated in both directions (from seed to target and vice versa), and these values were subsequently averaged. To obtain a measure of connectivity probability between ROIs (analysis 2), we used this average number of streamlines per seed voxel reaching the target (Croxson et al. 2005), expressed as a proportion of all successful samples in all pairwise connections in both hemispheres (see also Croxson et al. 2005; Eickhoff et al. 2010). This normalization approach allowed for a comparison of connectivity probability across ROIs and across the 2 hemispheres (note that the pattern of connectivity results is not changed by this scaling step).

Differences between the connectivity probability to different targets were assessed for each seed ROI separately, using a repeated-measure analysis of variance (ANOVA) (Croxson et al. 2005) with the factors hemisphere and target ROI, calculated in SPSS 16.0 (www.spss.com). We applied a Greenhouse–Geisser correction for sphericity and used post hoc pairwise t-tests with the Bonferroni step-down (Holm) correction at a significance level of $P < 0.05$.

For group analyses, the probabilistic connectivity distribution maps from individual participants were thresholded at a 5% level (thus selecting all connections where more than 1250 of 25 000 samples passed). They were then binarized, transferred into MNI space using the nonlinear registration warpfield (cf. image processing above) and summed up across participants to obtain the connectivity probability map of the group.

For the analysis of tracts originating from face-responsive ROIs and passing through the white-matter bundles ILF and AF (analysis 3), our tracking procedure was as follows (see also Croxson et al. [2005]): First, to define each bundle in each individual, fiber tracking was initiated twice (from 2 ROIs placed on the tract trajectory) and all samples from a given tract-defining ROI were kept when they reached the other ROI (see preceding section above). The 2 resulting connectivity maps were thresholded at 10% (to keep the core of the white-matter bundles), and the sum of the thresholded maps in both directions was then binarized and used to delineate the individual white-matter tract. Finally, each of the 2 fiber bundles (ILF and AF) served as a new ROI to measure trajectories going to and from the functionally defined face-responsive ROIs (Croxson et al. 2005). By using a binarized tract ROI, this approach highlights all tracts that originate in the face-responsive ROI and merge with any part of the white-matter tract, without requiring the fibers to be tracked along the whole tract and thus provides a high sensitivity to identify pathways between the tract and a target ROI. The procedure used to quantify connection probability was the same as used for the analysis between ROI pairs in analysis 2 (see above).

For all analyses, a manually drawn exclusion mask of the cerebellum was created for every participant in order to prevent aberrant paths from ventral brain areas (e.g., occipito-cerebellar shortcuts).

Results

We first performed a standard localizer fMRI session (Kanwisher et al. 1997; Pourtois et al. 2005a) to identify the functional network of face-responsive regions in each participant ($n = 22$) and then used the individually defined clusters of cortical activations as seed regions for probabilistic diffusion tensor tractography (see Materials and Methods and Table 1). All regions typically observed in previous studies of face perception were successfully identified (Fig. 1). We then analyzed connectivity between the core regions of the face-responsive network (FFA, OFA, and STS) and included the PCC and amygdala (AMG), 2 key regions of the extended system involved in face processing (Gobbini and Haxby 2007), plus the early visual cortex (CAL) serving as an additional control ROI. Three separate analyses of tractography were carried out to probe connectivity in this bilateral neural network, as described below.

Global Connectivity Pattern of Each ROI (analysis 1)

In analysis 1, we mapped the global probabilistic connectivity pattern for each face-responsive ROI, sending out 25 000 streamline samples from every voxel of each ROI, without any restriction. Figure 2 shows whole-brain maps where at least 1250 of these 25 000 streamline samples passed (threshold 5%) and overlapped in at least 11 participants (50%). Visual inspection of these maps (in relation to anatomical templates) indicated that, for FFA and OFA, the main connections ran through the ILF and the inferior fronto-occipito fasciculus (IFOF) toward the anterior temporal and inferior frontal areas, with only the OFA extending further into the orbitofrontal region. By contrast, the main connections of STS passed through different pathways in the AF and via SLF reaching more lateral prefrontal areas. PCC connected to the anterior cingulum bundle, the posterior cingulum, and parahippocampal region, as well as the precuneus. The amygdala (AMG) strongly projected to occipital regions via the ILF and through the uncinate fasciculus projected to orbitofrontal regions. Its connections through the fornix are probably indirect through the anterior commissure. Finally, the early visual ROI (CAL) showed prominent connections with the optic radiation and the splenial interhemispheric connection pathways but also projected densely via ILF and IFOF to the anterior temporal regions and (via IFOF) to orbitofrontal regions. Note that the spheres of the CAL-ROI were grown into subcortical white matter and did not exclusively comprise projections from striate but also from adjacent extrastriate areas, which explains the connection via IFOF. It is not always possible to separate ILF and IFOF in occipito-temporal regions, but only IFOF enters the external capsule and reaches orbitofrontal areas (Wakana et al. 2007; Catani and Thiebaut de Schotten 2008). However, the exact definition of ILF and IFOF are still debated in anatomic literature (Schmahmann and Pandya 2006).

Nevertheless, these results demonstrate that pathways could be reliably tracked from each of our ROIs and highlight distinct networks of long-range interconnections for each of the face-responsive areas. This differential pattern of connectivity between face-responsive ROIs is further illustrated in Figure 3, in which the whole-brain probabilities of distant projections to the cortical surface was computed from seeds in OFA, FFA, and STS in each individual (cf. also Fig. 2). Although purely descriptive, these data show that despite expected proximity
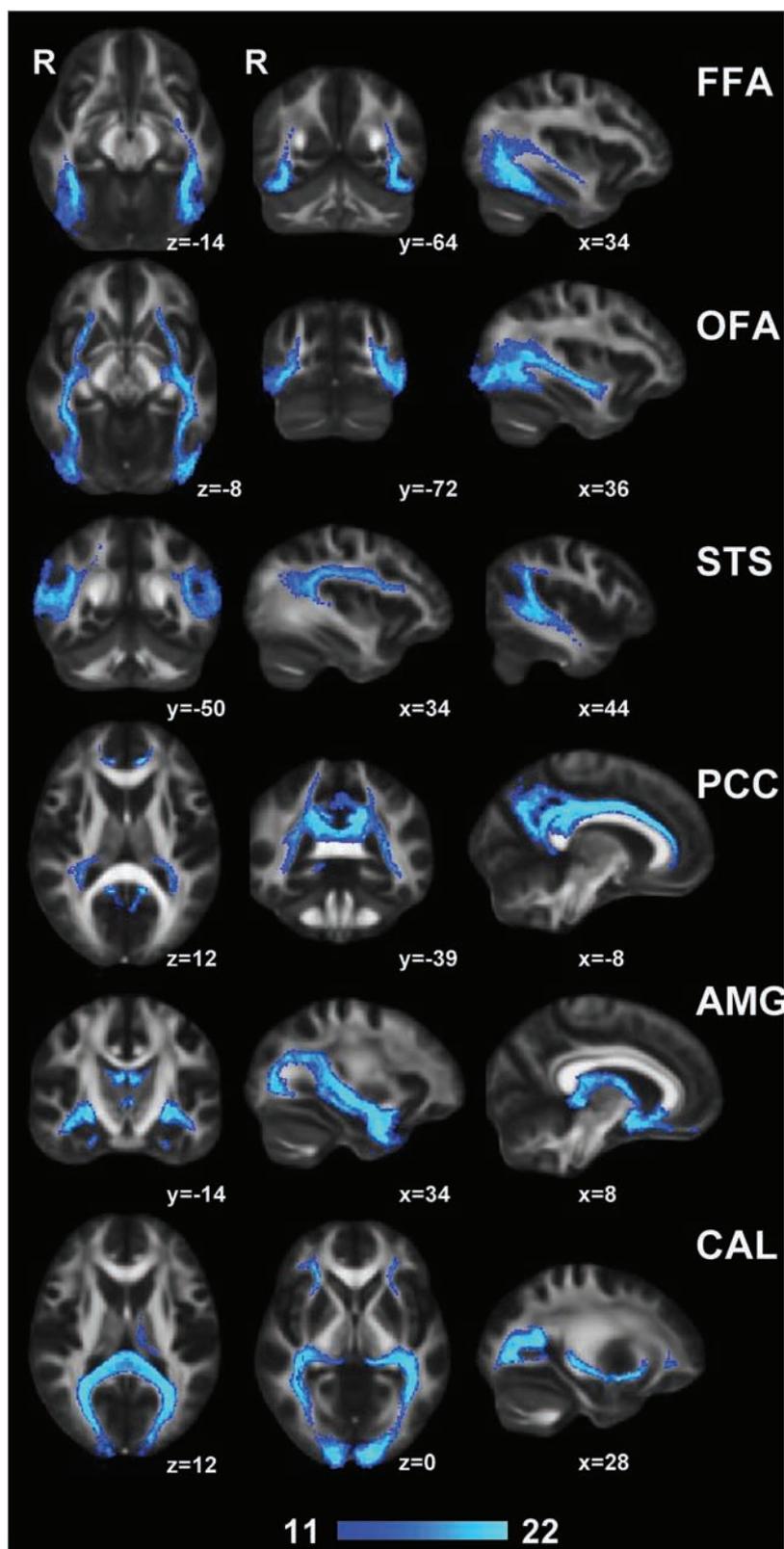
Figure 2. Global white-matter connectivity probability of each ROI (analysis 1). The distribution of white-matter projections across the whole brain is illustrated in axial, coronal, and sagittal views, as defined at the group level (22 participants) based on seeds from each of the individually defined ROIs (FFA, OFA, STS, PCC, AMG, and CAL). Whole-brain maps show all voxels, overlapping in at least 11 of 22 participants with the highest connectivity probability (>5% of all samples passing there) from each of the individually defined ROI.

biases that are inherent to DTI tractography (strong connections with adjacent cortical areas), the projections from OFA highlighted a "hotspot" in ventral temporal cortex partly overlapping with the FFA, whereas conversely the projections from FFA reached lateral occipital areas partly overlapping with OFA. STS showed distinct connections reaching lateral frontal
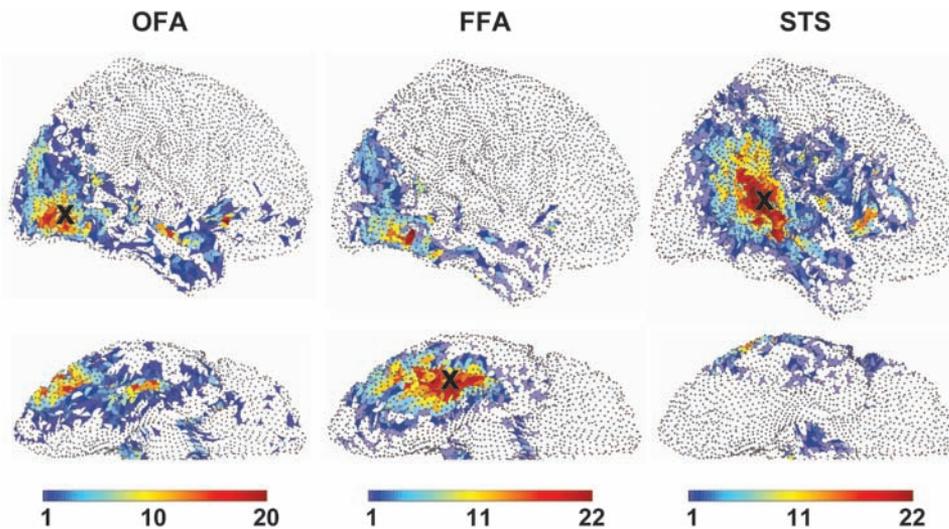
Figure 3. Whole-brain cortical connectivity probabilities for the 3 main face-responsive areas (analysis 1). For illustrative purpose, the endpoints of streamlines sent from each functionally defined seed ROI (see Fig. 1) were projected on a representation of the cortical surface abutting the white matter. Color range indicates the degree of between-participant overlap (right hemisphere view). Upper row: lateral views. Lower row: ventral views. Besides predominant connections with neighboring areas (proximity bias), each ROI disclosed additional projections to a few distant areas. Left: The OFA seed showed projections to ventral temporal areas corresponding to FFA (plus more anterior regions in temporal pole and frontal lobe). Middle: Vice versa, the FFA seed showed projections to lateral occipital areas corresponding to OFA. Right: STS showed no evidence for projections to occipital or temporal cortex (neither OFA or FFA), but some connections with more distant areas in lateral frontal cortex.

and superior parietal areas (i.e., in far distance) but no apparent hits in occipital or temporal areas (despite similar or even shorter distance).

Connectivity between all Pairs of ROIs (analysis 2)

In analysis 2, we quantified the connectivity probabilities between all pairs of face-responsive ROIs within each hemisphere, for each individual participant. From each seed ROI, we sent out 25 000 streamline samples and counted those that passed through the target ROI. We calculated the connectivity between the seed and target ROIs in both directions (using both ROIs of each pair once as seed and once as target; see Materials and Methods).

Figure 4 shows these connection probabilities between each pair of ROI (within one hemisphere or across both). For each seed ROI, a 2 × 5 repeated-measure ANOVA was performed on the connectivity values (across both hemispheres), with the factors of 2 hemispheres and 5 targets (Greenhouse–Geisser corrected if necessary). Post hoc comparisons were done by pair-wise t-tests using the Bonferroni step-down (Holm) correction at a significance level of $P < 0.05$.

For FFA, the streamlines in both hemispheres were directly connected to OFA with the highest probability relative to all other ROIs ($F_{1.01,21.24} = 128.98$, $P < 0.0001$). There was also a significant hemispheric asymmetry ($F_{1,21} = 5.93$, $P < 0.05$) in favor of the right side, with a further interaction ($F_{1.00,21.09} = 6.067$, $P < 0.05$) indicating that this difference was due to a stronger connectivity probability between FFA and OFA in the right than in the left hemisphere (Fig. 4).

For OFA, the results also showed a significant difference between the target regions ($F_{1.28,26.81} = 56.05$, $P < 0.0001$) with the strongest connectivity to FFA. There was again a predominance of the right hemisphere ($F_{1,21} = 6.81$, $P < 0.05$) and an interaction ($F_{1.43,30.11} = 4.67$, $P < 0.01$), reflecting higher connection probability between OFA and FFA on the right side, as compared with all other pairs.

For STS, we found no significant difference for connectivity probability with the target ROIs ($P = 0.37$) and no asymmetry between hemispheres ($P = 0.66$). Thus, STS showed a low probability of direct connections to all face-responsive ROIs, with no preferential link to FFA or OFA compared with any of the tested ROIs (including the control region in early occipital cortex, CAL).

For PCC, there was also a low probability of connections to all other ROIs, with no hemispheric difference ($P = 0.22$), and no difference between the target regions ($P = 0.33$).

For AMG, there was no hemispheric difference, but a strong effect of ROIs ($F_{1.12,23.53} = 21.65$, $P < 0.0001$), reflecting a significantly higher connectivity probability with CAL compared with every other ROI in both hemispheres (all post hoc pairwise t-tests, $P < 0.05$).

Finally, the CAL seed ROI showed no hemispheric difference but a strong effect of target ROIs ($F_{1.50,31.43} = 34.21$, $P < 0.01$), with post hoc comparisons revealing significant differences in connectivity for the AMG relative to every other ROI on the left side, as well as for the OFA and AMG relative to other ROIs in the right hemisphere ($P < 0.05$).

To summarize, these results support the existence of a strong direct white-matter connectivity between OFA and FFA, significantly more developed in the right than in the left hemisphere. They also point to high connectivity between the amygdala (AMG) and early visual areas (CAL) and OFA. However, the connections to and from STS within this network of face-responsive areas were globally weak, despite the fact that long-range trajectories were successfully mapped from this ROI in analysis 1 (Fig. 2). This finding might either reflect the fact that trajectories from the face-responsive STS region are in generally difficult to track due to many fibers crossings around this region or that STS indeed is not "directly" connected to any of the other ROIs within the functionally defined face-responsive network (see next sections and Discussion).

left - hemisphere - right
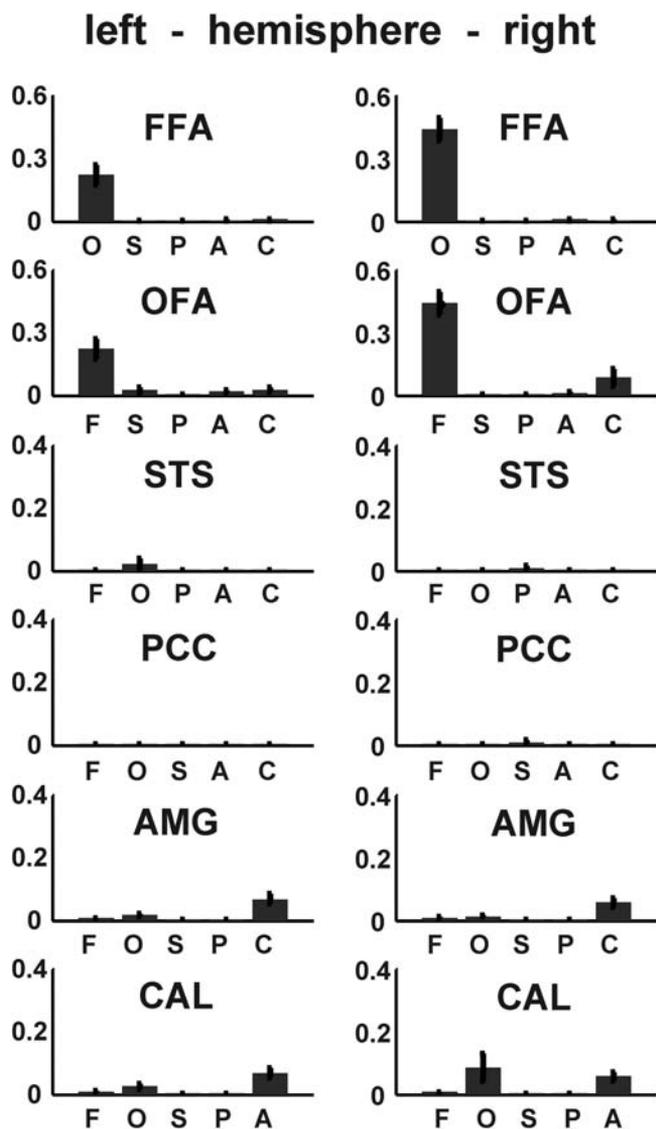
Figure 4. Connectivity probability between each pair of ROIs (analysis 2). Each panel represents a seed ROI and its connectivity to the other 5 (target) ROIs. Left panel shows left hemisphere, right panel shows right hemisphere (F = FFA, O = OFA, S = STS, P = PCC, A = AMG, C = CAL). Connectivity probability is indicated as a proportion of the sum of all pairwise connections in both hemispheres, permitting for a comparison of the pairwise connections both across ROIs and across hemispheres. The error bar indicates the standard error.

Connectivity between Each ROI and Major White-Matter Bundles (analysis 3)

Analysis 3 was carried out in order to test for fiber connections originating from each face-responsive ROI and passing through parts of the major white-matter bundles that link visual areas with other distant brain regions. For this purpose, we focused on the ILF and the AF because these 2 tracts interconnect widely between the occipital, temporal, and parietal cortices (Catani et al. 2003; Rilling et al. 2008). This analysis should also rule out that the weak connectivity probability of STS with FFA and OFA was related to an intrinsic bias of the tracking algorithm that would prevent streamlines from STS to establish any connectivity with other regions due the proximity of fiber tracts or abundant crossing fibers adjacent to STS (even though we used a probabilistic model that estimated 2 fiber directions; see

Materials and Methods). We first defined ILF and AF in each individual according to standard procedures (Wakana et al. 2007; Rilling et al. 2008) (see Materials and Methods and Fig. 5) and then estimated the probability of fibers passing from the face-responsive ROI to any part of the tracts. Connectivity probability was again expressed proportionally to the sum of all connections involving both homotopic ROIs in both hemispheres.

Figure 6 shows the connectivity probability of each face-responsive ROI with the ILF and the AF. As above, we performed repeated-measure ANOVAs on the reciprocal connectivity values of each tract, using 6 ROIs and 2 hemispheres as separate factors.

The ILF showed no hemispheric asymmetry, but a strong effect of target ROI ($F_{1.98,41.70} = 97.80$, $P < 0.0001$), reflecting significantly more connections to AMG and CAL than to all other ROIs on both sides (see Fig. 6) and more connections to FFA and OFA than STS and PCC (post hoc comparisons $P < 0.05$). In contrast, the AF showed a main effect of ROI ($F_{1.67,35.08} = 155.65$, $P < 0.0001$) that reflected a greater connectivity to STS than to all other ROIs in both hemispheres, but also an interaction of ROI × hemisphere ($F_{1.32,27.63} = 9.80$, $P < 0.01$) indicating a significantly higher connection probability of STS to AF in the right than in the left hemisphere. These findings thus converge with the above pairwise analysis and indicate that OFA, FFA, AMG, and CAL all preferentially connect to pathways passing through the ILF, whereas STS has a distinct connectivity pattern with pathways passing via the AF and only weak direct links to the ILF.

Taken together, these results reveal that CAL, OFA, and FFA participate in the same cortico-cortical network associated with ILF and moreover suggest that few trajectories project downwards from STS to the inferior temporal lobe even though this region is located laterally on the surface of the temporal lobe, close to the ILF. Instead, the main connectivity of STS is directed to anterior and superior temporal areas, as well as to the parietal and frontal lobes.

### Microstructural Characteristics of Fiber Tracts (analysis 4)

Finally, we extracted microstructural properties of the white matter (Pierpaoli et al. 1996), including the mean FA and mean diffusivity (MD) for the most significant connections identified in previous analyses (OFA-FFA pathways and AMG-CAL pathways), plus AF and ILF, in each hemisphere and for each participant. Table 2 shows the mean values (and SD) for these connections, averaged for both fiber-tracking directions. All these values were in the range typically reported for white-matter tracts (Wahl et al. 2010), thus supporting the quality and reliability of our data.

For FA, a 2 (hemisphere) × 4 (tract type) ANOVA revealed a strong effect of tract type ($F_{2.27,47.69} = 187.002$, $P < 0.0001$), reflecting the fact that FA values were lower for pathways connecting OFA and FFA than others ($P < 0.0001$, Bonferroni corrected), consistent with a less homogenous fiber pathway, probably due to local fibers crossing in the proximity of cortical gray matter and gyri; however, there was no difference between pathways connecting CAL and AMG and the major fiber bundles (AF and ILF). A significant interaction between tract type and hemisphere ($F_{2.32,48.75} = 3.94$, $P < 0.05$) indicated an asymmetry only for the AF in favor of the left hemisphere ($P < 0.05$, Bonferroni corrected).

The same analysis for MD, again revealed a main effect of tract ($F_{1.39,29.26} = 43.96$, $P < 0.0001$), but no interaction, indicating that values were the highest for the pathways
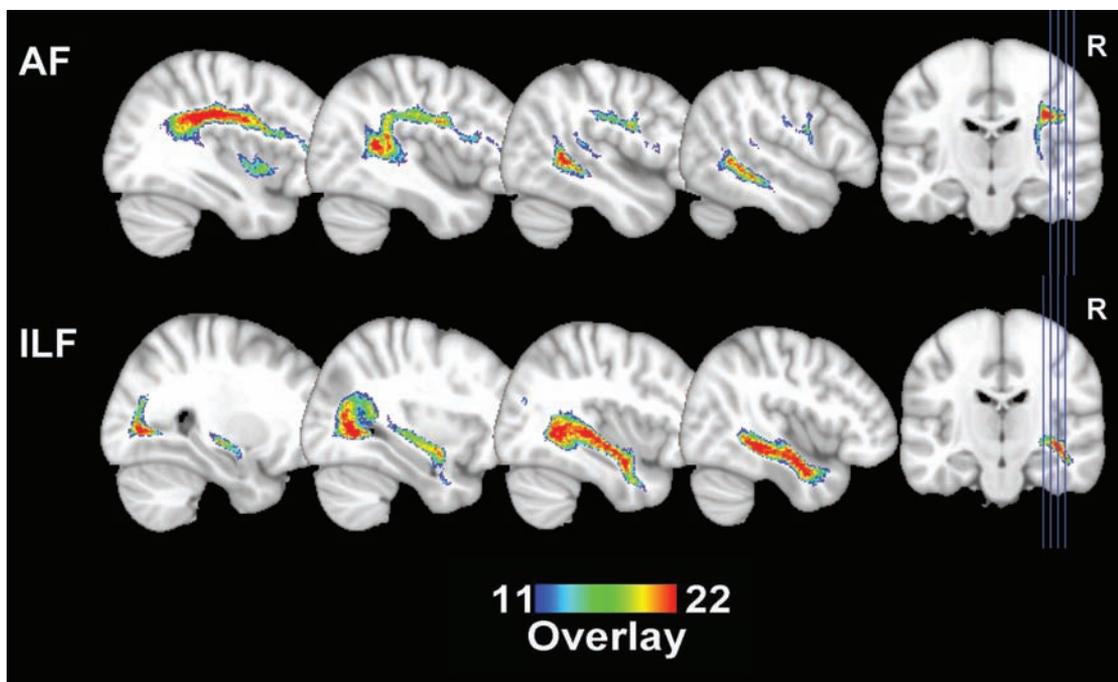
Figure 5. ILF and AF. AF and ILF were determined by fiber tracking in each individual. Whole-brain maps show all voxels with >10% probability to belong to the tract in more than 11 of 22 participants (the color codes the degree of overlap between the participants). These tracts are subsequently taken to probe connectivity to the face-responsive regions (see Fig. 6).
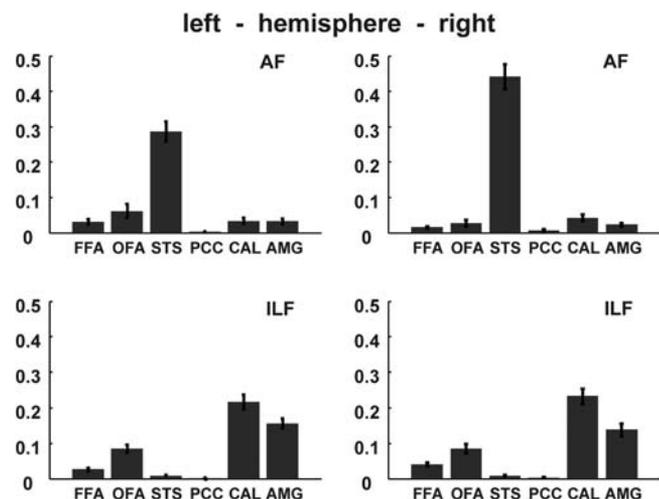
Figure 6. Connectivity probabilities between major white-matter bundles and face-responsive regions (analysis 3). Each panel represents the connectivity probability from the AF and the ILF toward each of the face-responsive ROIs (F = FFA, O = OFA, S = STS, P = PCC, A = AMG, C = CAL). The connectivity probability is expressed as a proportion of all connections in both hemispheres, thus permitting comparison across hemisphere. The error bar indicates the standard error.

Table 2

Microstructural properties of fiber tracts

	FA	MD
Left OFA-FFA	0.331 (0.042)	0.751 (0.038)
Right OFA-FFA	0.330 (0.043)	0.743 (0.036)
Left AMG-CAL	0.450 (0.034)	0.849 (0.112)
Right AMG-CAL	0.454 (0.027)	0.828 (0.049)
Left AF	0.464 (0.026)	0.713 (0.020)
Right AF	0.436 (0.048)	0.738 (0.039)
Left ILF	0.470 (0.018)	0.775 (0.024)
Right ILF	0.466 (0.023)	0.790 (0.025)

Note: Microstructural properties of the most significant connections of face-responsive regions. Values are averaged for fiber tracking in both directions. FA is dimensionless, MD is given in the unit of 10^{-3} mm^2/s.

between CAL and AMG, followed by the ILF ($P < 0.05$) and the pathways between OFA and FFA (only significant for the right hemisphere, $P < 0.00001$), while pathways of the AF showed the lowest values ($P < 0.0001$; all Bonferroni corrected).

Discussion

Our study used DTI tractography to examine for the first time the pattern of structural connectivity between cortical areas involved in face processing in humans (Fig. 7). We found a high

probability of direct interconnections between OFA and FFA, with a marked predominance in the right hemisphere. We also found direct connectivity between early visual areas and the amygdala, whereas the connection probability between OFA or FFA and amygdala was much weaker. In addition, we found that STS was not preferentially connected to FFA, neither to OFA, but rather linked to more anterior temporal, superior parietal, and even frontal regions. Although it is not possible to distinguish between afferent and efferent connections because DTI-based tractography cannot visualize neuronal directionality, these findings provide important constraints for future models of face perception in humans. In the following, we discuss each result separately.

The high connectivity between FFA and OFA with a right hemisphere predominance is highly consistent with results from imaging studies and neuropsychology (Grüsser and Landis 1991; Kim et al. 2006; Vuilleumier 2007; Fox et al. 2008; Thomas et al. 2009), suggesting that these 2 visual areas entertain very close interactions to subserve face categorization and identification
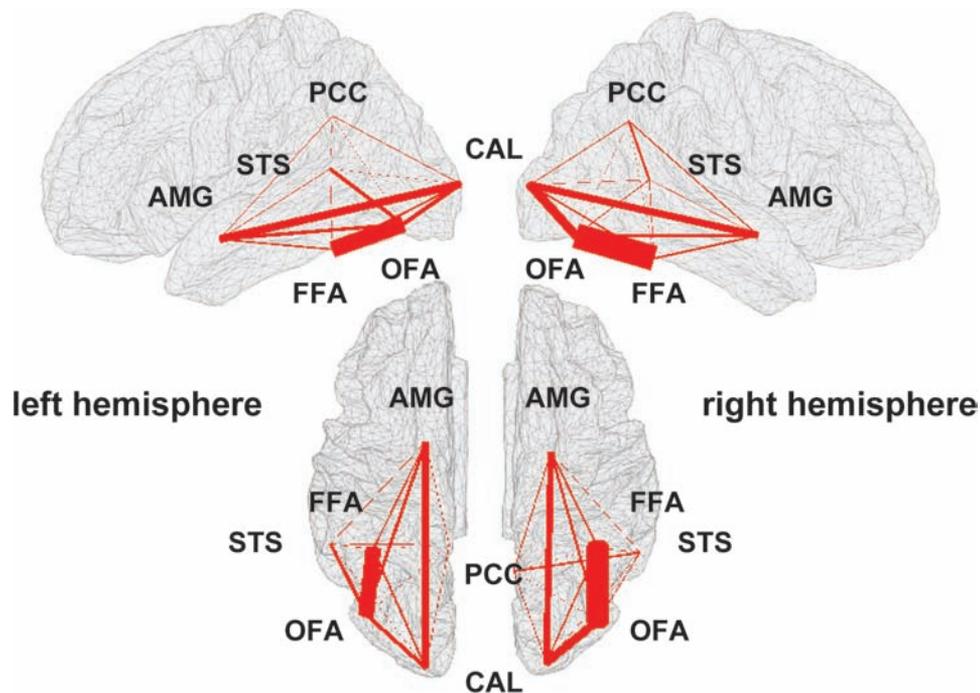
Figure 7. Summary of the main white-matter connectivity results. Connectivity results are shown for both hemispheres, averaged across 22 participants. The width of each connection path reflects their relative connectivity probability (averaged for streamlines to and from each ROI in each pair). A proportional contrast weight is applied to the path width for illustration purposes (linear = 4, gamma = 0.5).

(Sorger et al. 2007). In turn, the OFA showed relatively stronger connectivity with early visual cortex than the FFA, consistent with a hierarchical organization from posterior occipital to more anterior temporal areas and converging with recent neurocognitive models (Haxby et al. 2000; Gobbini and Haxby 2007) and functional analyses using dynamic causal modeling (Fairhall and Ishai 2007) or resting state connectivity (Zhu et al. 2011). These findings support the view that OFA and FFA work in concert during face recognition and that damage to either both areas or their interconnections may cause severe prosopagnosia (Rossion et al. 2003; Fox et al. 2008). Likewise, the hemispheric asymmetry of connectivity probability between OFA and FFA (and also between CAL and OFA) in favor of the right side accords with the well-known right hemisphere dominance for face processing network as revealed by functional neuroimaging, lesion studies, and split-hemifield experiments (Grüsser and Landis 1991; Kanwisher et al. 1997; Rossion et al. 2003; Fox et al. 2008). Furthermore, the connectivity probability of STS with the AF system was also higher in the right hemisphere. Hemispheric asymmetries have been reported for other white-matter tracts, especially in terms of microstructural properties and typically related to other lateralized functions such as language and attention (for a review, see Thiebaut de Schotten et al. 2011). However, it is important to keep in mind that such asymmetry in connectivity probability may have multiple reasons, including lower FA values due to more complex fiber organization or larger tracts due to handedness, gender, or age factors (our participants were young, balanced across genders, and all right handed, in order to control for these factors).

Finally, the strong connectivity between early visual areas (CAL) and amygdala (AMG) adds to recent findings by DTI (Catani et al. 2003; Pugliese et al. 2009), fMRI (Vuilleumier

et al. 2004), and magnetoencephalography studies (Rudrauf et al. 2008), suggesting that anterior temporal lobe structures may receive direct visual inputs from striate and extrastriate cortex via long-range fiber tracts. It has been hypothesized that these direct pathways serve both the rapid bottom-up registration of emotionally significant stimuli in the amygdala and top-down modulatory feedback from temporal limbic areas on posterior cortical regions (Amaral 2002; Vuilleumier et al. 2004). Our results also add to previous tractography studies of the amygdala that focused on connections with temporal pole and OFC (Bach et al. 2011).

Our finding that the white-matter connection probability of the amygdala was higher with occipital cortex (CAL) than with FFA is interesting for 2 reasons. First, this result suggests that the existence of direct white-matter pathways from occipital cortex to the amygdala partly bypassing the FFA, consistent with the fact that in humans the amygdala is not only linked to the core face processing network (Gobbini and Haxby 2007) but also recruited more generally during visual processing to monitor the affective relevance of incoming stimuli (Vuilleumier 2005; Bar and Neta 2007). Second, our results support the notion that the detection of emotionally relevant face information may take place in the amygdala independent of the degree of processing in FFA (Whalen et al. 1998; Vuilleumier et al. 2001; Peelen et al. 2009). For example, amygdala responses to faces arise after short latencies (~120 ms), that is, 50 ms prior to cortical responses typically associated with face recognition (~170 ms; see Pourtois et al. 2010b). This early amygdala activation may allow feedback influences on ongoing cortical processing, including on V1 (Rotshtein et al. 2010), through direct reciprocal projections from the amygdala to the occipital cortex.

We found that PCC had a low probability of direct connections to all other face-responsive regions, but strong projections to both the anterior and posterior cingulum bundles the parahippocampal region, as well as the precuneus. This connectivity pattern agrees with results of histological studies (Vogt and Pandya 1987), showing a similar dichotomy of connections to ACC and to parahippocampal regions. Although often responsive to faces, the exact role of PCC remains unclear and generally attributed to memory, familiarity, and social or affective saliency (Pourtois et al. 2005b; Gobbini and Haxby 2007; Vrticka et al. 2009). PCC is thus part of the extended face network, and its connections with the core face-responsive areas might arise via its projections to orbitofrontal areas and medial temporal lobe (see Fig. 2), implicated in the evaluation of self-relevance and contextual memory information, respectively (Vogt et al. 2006). This multisynaptic relay might account for the lack of direct connections between PCC and visual regions showing concomitant activations in the face localizer scan, such as FFA, OFA, or STS.

Importantly, our results concerning connectivity of the face-responsive STS cannot easily be reconciled with classic theoretical accounts of face processing. Contrary to the predictions of current cognitive models (Haxby et al. 2000; Gobbini and Haxby 2007) and functional DCM results (Fairhall and Ishai 2007), we did not find any direct anatomical white-matter pathway between STS and FFA nor between STS and OFA.

It should be noted that the inability to trace a pathway with DTI cannot be taken, in itself, as definitive evidence that the pathway does not exist (Johansen-Berg and Rushworth 2009) but needs confirmation or convergence with other data. A weak connectivity between STS and extrastriate visual areas could arise from the fact that the large fiber tract of the ILF (with a dominant posterior–anterior direction) hampered the tracking of fibers from/to STS due to their superior–inferior direction across the temporal lobe. However, by measuring the projections from STS that reached either ILF or AF in another independent analysis (analysis 3), we found that pathways from the STS region were prominently related to the AF system but only poorly connected to the ILF system. Therefore, our results may suggest the existence of 2 distinct networks within the temporal lobe: a ventral pathway is related to the ILF, extending from occipital to anterior temporal cortex, and located in the inferior and medial parts of the temporal lobe; whereas another more dorsal system is related to the AF, extending through the SLF between the frontal and superior temporal cortex and located in the more superior and lateral part of the temporal lobe (see Figs 2 and 5).

As mentioned in the Materials and Methods section, we used fMRI peaks as seeds for fiber tracking, which might produce unknown biases in the results. The reliability of fMRI activations is variable, with the right FFA generally showing the most consistent response in all participants, but other regions such as left STS or left OFA often show a higher degree of interindividual variability. Several different approaches have been used to localize ROIs and to cope with these interindividual differences (for review, see Fox et al. 2009). Many imaging studies rely on group-level analysis using normalized brain anatomy, sometimes leading to activations that are not consistently found in each and every subject of the group and because the peak represents an average result, it may not provide the exact localization of maximal responses in individual brains. Another approach (chosen here) is to vary the statistical threshold at which a ROI is identified in each individual brain. This is, however, marred with the noncorrection of multiple comparisons and with the problem that applying lower thresholds also increases the size of clusters. These issues motivated our approach to define seed ROIs with spheres of similar size, centered on the peak of activations in the face localizer. This approach is consistent with a large body of neuroimaging research on face processing that used similar approaches to define functional ROIs (Saxe et al. 2006; Fox et al. 2009) and seems unlikely to introduce biases in our DTI results.

It is also important to stress that fiber-tracking algorithms (in individual participants) cannot go beyond the MRI voxel resolution, which is much coarser than the actual size of neuronal structures. Hence, this technique does not allow the visualization of small pathways between very specific cortical sites and distant targets. This general limitation of DTI may prevent definite conclusions about selective connections of some regions where many functionally distinct pathways may converge or cross but overlap in a single voxel. For this reason, DTI tractography reveals only probabilistic connectivity through major pathways but not real and complete anatomical connectivity.

Nevertheless, it is important to note that our results for STS accord with several anatomical tracer studies in the macaque brain, which also demonstrated selective connections of STS with regions of the frontal and temporal lobes but not with extrastriate visual areas. STS is known to be a polysensory region (Beauchamp et al. 2008) that is widely connected with various brain areas but with a distinctive connectivity patterns of each subregion within STS (Seltzer and Pandya 1978). For example, tracer studies have revealed selective connections of different parts of STS to the retrosplenial cortex (Seltzer and Pandya 2009), parahippocampal cortex (Seltzer and Pandya 1994), inferior parietal lobe (Cavada and Goldman-Rakic 1989; Seltzer and Pandya 1994), frontal lobe (Padberg et al. 2003), postrolandic cortex (Seltzer and Pandya 1994), and basal ganglia (Yeterian and Pandya 1998). However, only the very rostral part of STS (TPO-1) has been found to receive inputs from inferotemporal regions and only indirectly via TEa and IPa (Seltzer and Pandya 1994). Hence, no direct connections appear to exist between STS and visual areas in inferior temporal cortex in primates, as explicitly noted by several anatomical studies (Streitfeld 1980; Seltzer and Pandya 1994; Saleem et al. 2000) (only one case of injections to the superior bank of the STS shows a connection to OTS, the animal region which is phylogenetically closest to the human FFA [Case 9, Schmahmann and Pandya 2006]. However, other studies have not found this connection from comparable injection sites [Cases 10, 11, 23, 24, 25, Seltzer and Pandya 2009]). Our fiber-tracking results for the face-responsive STS region are therefore in line with these tracer studies, corroborating the anatomical evidence for only weak direct connectivity between STS and FFA or OFA but they contrast with traditional neurocognitive models of face processing. This convergence of findings across methods and species provides additional support to our DTI results.

More generally, our structural results may help explain some findings in functional imaging studies and refine face processing models in humans. For example, many fMRI studies have reported that STS tends to show a response pattern different from FFA and OFA (Pourtois et al. 2005a; Ewbank and Andrews 2008). Such differences have usually been attributed to a dissociation between 1) the processing of invariant facial information that is used for recognition of identity (involving

FFA and OFA) and 2) the analysis of changeable aspects of faces (involving STS), such as eye gaze and facial expression (Puce et al. 1998; Hoffman and Haxby 2000), which are important for social and emotional communication (Haxby et al. 2000). Our finding that STS is preferentially connected to the AF fiber network, rather than to the ILF network, unlike the other visual areas within the core face processing system, adds further evidence in support of its distinct functional role. It is likely that STS receives visual inputs from motion-sensitive areas and neighboring extrastriate cortical regions (rather than from OFA or FFA) to subserve the processing of face expression and gaze information (see Ethofer et al. 2011). This would accord with tracer studies in primates (Seltzer and Pandya 1989; Baizer et al. 1991; Seltzer et al. 1996) and appears consistent with the involvement of STS subregions in biological motion processing (Nelissen et al. 2006). Moreover, imaging studies in primates suggest that at least 2 different visual paths might reach STS besides V5/MT (Nelissen et al. 2006), but further research is necessary to verify this notion in humans by combining fMRI and DTI as here. The fact that STS was activated by static images of faces in our study is consistent with many previous reports (e.g., Puce et al. 1998; Hoffman and Haxby 2000), even though it is known that dynamic face stimuli elicit stronger and more reproducible pSTS activation (e.g., Fox et al. 2009). Moreover, both MT/V5 and STS regions respond to static images of implied motion (e.g., Kourtzi and Kanwisher 2000; Jellema and Perrett 2003; Nelissen et al. 2006). Taken together, these findings indicate that STS might preferentially extract motion cues and contribute to higher level social processes recruited during face perception, such as the representation of mental states or attribution of intentions (Allison et al. 2000; Blakemore et al. 2004), which, in turn, may rely on selective interactions with frontal and parietal areas mediating executive functions, attention, or mentalizing. Accordingly, other findings suggest that the right STS shows both structural and functional connectivity with the inferior frontal cortex that underlie attentional responses to perceived eye gaze contact in faces (Ethofer et al. 2011).

It is worth noting that our structural data only partly replicates the patterns of functional connectivity previously suggested by dynamic causal modeling during fMRI (Fairhall and Ishai 2007). This study showed strong connections between OFA and STS and between OFA and FFA but no direct connection between FFA and STS. Our DTI results accord with the 2 latter pathways but not with the former. Another fMRI study showed strong OFA-FFA connectivity during resting state but did report connectivity with STS (Zhu et al. 2011). However, functional connectivity as measured by DCM and other correlation techniques (such as psychophysical interactions, see Ethofer et al. 2011) may reflect both direct structural pathways (measured by DTI) and multi-synaptic links (underlying coherent activity without direct input transmission). Likewise, functional connectivity results have shown a coupling of the right inferior frontal gyrus with both the FFA (Fairhall et al. 2011) and STS (Ethofer et al. 2011) during face processing but only the latter seems to be mediated by direct structural pathways (see Ethofer et al. 2011).

In summary, we combined functional MRI during a face localizer task to identify a network of face-responsive regions in individual subjects with diffusion tensor probabilistic tractography to establish the white-matter connectivity between regions within this network. Although we demonstrate direct pathways between early visual areas and OFA, between

OFA and FFA, and between occipital visual areas and AMG, we did not find evidence for any preferential connectivity between OFA and STS nor between FFA and STS. We suggest that extrastriate visual areas and amygdala are interconnected in a common network centered on the ILF, whereas the face-responsive STS region belongs to a distinct network centered on the AF, with only weak connections to the ILF. The lack of direct connectivity of STS with FFA or OFA implies that the role of STS is dissociable from more coordinated computations in the FFA and OFA during face recognition, presumably related to higher level aspects of social cognition rather than strictly visual processes. Future studies should further explore the nature of functional dissociations between these distinct networks and probe for the temporal dynamics of interactions between face-responsive regions by combining fMRI with time-resolved techniques such as electroencephalography or intracranial recordings. These data also provide an important step for further work on disorders of visual and social cognition, such as prosopagnosia and autism. More generally, our study demonstrates that fMRI and DTI can be fruitfully integrated to gain a more complete understanding of functional brain networks, beyond the traditional mapping approaches based on functional activations alone.

Notes

Preliminary results of this study were reported at the Society for Neuroscience Meeting 2009, Chicago. *Conflict of Interest*: None declared.

References

Allison T, Puce A, McCarthy G. 2000. Social perception from visual cues: role of the STS region. Trends Cogn Sci. 4:267–278.

Amaral DG. 2002. The primate amygdala and the neurobiology of social behavior: implications for understanding social anxiety. Biol Psychiatry. 51:11–17.

Amaral DG, Behniea H, Kelly JL. 2003. Topographic organization of projections from the amygdala to the visual cortex in the macaque monkey. Neuroscience. 118:1099–1120.

Ashburner J, Friston KJ. 2005. Unified segmentation. Neuroimage. 26:839–851.

Bach DR, Behrens TE, Garrido L, Weiskopf N, Dolan RJ. 2011. Deep and superficial amygdala nuclei projections revealed in vivo by probabilistic tractography. J Neurosci. 31:618–623.

Baizer JS, Ungerleider LG, Desimone R. 1991. Organization of visual inputs to the inferior temporal and posterior parietal cortex in macaques. J Neurosci. 11:168–190.

Bar M, Neta M. 2007. Visual elements of subjective preference modulate amygdala activation. Neuropsychologia. 45:2191–2200.

Beauchamp MS, Yasar NE, Frye RE, Ro T. 2008. Touch, sound and vision in human superior temporal sulcus. Neuroimage. 41:1011–1020.

Behrens TE, Berg HJ, Jbabdi S, Rushworth MF, Woolrich MW. 2007. Probabilistic diffusion tractography with multiple fibre orientations: what can we gain? Neuroimage. 34:144–155.

Behrens TE, Woolrich MW, Jenkinson M, Johansen-Berg H, Nunes RG, Clare S, Matthews PM, Brady JM, Smith SM. 2003. Characterization and propagation of uncertainty in diffusion-weighted MR imaging. Magn Reson Med. 50:1077–1088.

Blakemore SJ, Winston J, Frith U. 2004. Social cognitive neuroscience: where are we heading? Trends Cogn Sci. 8:216–222.

Calder AJ, Beaver JD, Winston JS, Dolan RJ, Jenkins R, Eger E, Henson RN. 2007. Separate coding of different gaze directions in the superior temporal sulcus and inferior parietal lobule. Curr Biol. 17:20–25.

Catani M, Howard RJ, Pajevic S, Jones DK. 2002. Virtual in vivo interactive dissection of white matter fasciculi in the human brain. Neuroimage. 17:77–94.

Catani M, Jones DK, Donato R, Ffytche DH. 2003. Occipito-temporal connections in the human brain. Brain. 126:2093–2107.

Catani M, Mesulam M. 2008. The arcuate fasciculus and the disconnection theme in language and aphasia: history and current state. Cortex. 44:953–961.

Catani M, Thiebaut de Schotten M. 2008. A diffusion tensor imaging tractography atlas for virtual in vivo dissections. Cortex. 44(8): 1105–1132.

Cavada C, Goldman-Rakic PS. 1989. Posterior parietal cortex in rhesus monkey: II. Evidence for segregated corticocortical networks linking sensory and limbic areas with the frontal lobe. J Comp Neurol. 287:422–445.

Croxson PL, Johansen-Berg H, Behrens TE, Robson MD, Pinsk MA, Gross CG, Richter W, Richter MC, Kastner S, Rushworth MF. 2005. Quantitative investigation of connections of the prefrontal cortex in the human and macaque using probabilistic diffusion tractography. J Neurosci. 25:8854–8866.

Dauguet J, Peled S, Berezovskii V, Delzescaux T, Warfield SK, Born R, Westin CF. 2007. Comparison of fiber tracts derived from in-vivo DTI tractography with 3D histological neural tract tracer reconstruction on a macaque brain. Neuroimage. 37:530–538.

Dougherty RF, Ben-Shachar M, Bammer R, Brewer AA, Wandell BA. 2005. Functional organization of human occipital-callosal fiber tracts. Proc Natl Acad Sci U S A. 102:7350–7355.

Eickhoff SB, Jbabdi S, Caspers S, Laird AR, Fox PT, Zilles K, Behrens TE. 2010. Anatomical and functional connectivity of cytoarchitectonic areas within the human parietal operculum. J Neurosci. 30:6409–6421.

Ethofer T, Gschwind M, Vuilleumier P. 2011. Processing social aspects of human gaze: a combined fMRI-DTI study. Neuroimage. 55(1): 411–419.

Ewbank MP, Andrews TJ. 2008. Differential sensitivity for viewpoint between familiar and unfamiliar faces in human visual cortex. Neuroimage. 40:1857–1870.

Fairhall SL, Anzellotti S, Pajtas PE, Caramazza A. 2011. Concordance between perceptual and categorical repetition effects in the ventral visual stream. J Neurophysiol. 106:398–408.

Fairhall SL, Ishai A. 2007. Effective connectivity within the distributed cortical network for face perception. Cereb Cortex. 17:2400–2406.

Fox CJ, Iaria G, Barton JJ. 2008. Disconnection in prosopagnosia and face processing. Cortex. 44:996–1009.

Fox CJ, Iaria G, Barton JJ. 2009. Defining the face processing network: optimization of the functional localizer in fMRI. Hum Brain Mapp. 30:1637–1651.

Friston KJ, Fletcher P, Josephs O, Holmes A, Rugg MD, Turner R. 1998. Event-related fMRI: characterizing differential responses. Neuroimage. 7:30–40.

Gauthier I, Tarr MJ, Moylan J, Skudlarski P, Gore JC, Anderson AW. 2000. The fusiform "face area" is part of a network that processes faces at the individual level. J Cogn Neurosci. 12:495–504.

Gobbini MI, Haxby JV. 2007. Neural systems for recognition of familiar faces. Neuropsychologia. 45:32–41.

Grill-Spector K, Knouf N, Kanwisher N. 2004. The fusiform face area subserves face perception, not generic within-category identification. Nat Neurosci. 7:555–562.

Grüsser O-J, Landis T. 1991. Visual agnosias and other disturbances of visual perception and cognition. London: The Macmillan Press.

Hagmann P, Cammoun L, Martuzzi R, Maeder P, Clarke S, Thiran JP, Meuli R. 2006. Hand preference and sex shape the architecture of language networks. Hum Brain Mapp. 27:828–835.

Haxby JV, Hoffman EA, Gobbini MI. 2000. The distributed human neural system for face perception. Trends Cogn Sci. 4:223–233.

Hoffman EA, Haxby JV. 2000. Distinct representations of eye gaze and identity in the distributed human neural system for face perception. Nat Neurosci. 3:80–84.

Jellema T, Perrett DI. 2003. Cells in monkey STS responsive to articulated body motions and consequent static posture: a case of implied motion? Neuropsychologia. 41:1728–1737.

Johansen-Berg H, Rushworth MF. 2009. Using diffusion imaging to study human connectional anatomy. Annu Rev Neurosci. 32:75–94.

Kanwisher N, McDermott J, Chun MM. 1997. The fusiform face area: a module in human extrastriate cortex specialized for face perception. J Neurosci. 17:4302–4311.

Kim M, Ducros M, Carlson T, Ronen I, He S, Ugurbil K, Kim DS. 2006. Anatomical correlates of the functional organization in the human occipitotemporal cortex. Magn Reson Imaging. 24:583–590.

Kourtzi Z, Kanwisher N. 2000. Activation in human MT/MST by static images with implied motion. J Cogn Neurosci. 12:48–55.

Liu J, Harris A, Kanwisher N. 2002. Stages of processing in face perception: an MEG study. Nat Neurosci. 5:910–916.

Liu J, Harris A, Kanwisher N. 2010. Perception of face parts and face configurations: an FMRI study. J Cogn Neurosci. 22:203–211.

Makris N, Kennedy DN, McInerney S, Sorensen AG, Wang R, Caviness VS, Jr, Pandya DN. 2005. Segmentation of subcomponents within the superior longitudinal fascicle in humans: a quantitative, in vivo, DT-MRI study. Cereb Cortex. 15:854–869.

Nelissen K, Vanduffel W, Orban GA. 2006. Charting the lower superior temporal region, a new motion-sensitive region in monkey superior temporal sulcus. J Neurosci. 26:5929–5947.

Padberg J, Seltzer B, Cusick CG. 2003. Architectonics and cortical connections of the upper bank of the superior temporal sulcus in the rhesus monkey: an analysis in the tangential plane. J Comp Neurol. 467:418–434.

Peelen MV, Lucas N, Mayer E, Vuilleumier P. 2009. Emotional attention in acquired prosopagnosia. Soc Cogn Affect Neurosci. 4:268–277.

Pierpaoli C, Jezzard P, Basser PJ, Barnett A, Di Chiro G. 1996. Diffusion tensor MR imaging of the human brain. Radiology. 201:637–648.

Pourtois G, Spinelli L, Seeck M, Vuilleumier P. 2010a. Modulation of face processing by emotional expression and gaze direction during intracranial recordings in right fusiform cortex. J Cogn Neurosci. 22(9):2086–2107.

Pourtois G, Spinelli L, Seeck M, Vuilleumier P. 2010b. Temporal precedence of emotion over attention modulations in the lateral amygdala: intracranial ERP evidence from a patient with temporal lobe epilepsy. Cogn Affect Behav Neurosci. 10:83–93.

Pourtois G, Schwartz S, Seghier ML, Lazeyras F, Vuilleumier P. 2005a. Portraits or people? Distinct representations of face identity in the human visual cortex. J Cogn Neurosci. 17:1043–1057.

Pourtois G, Schwartz S, Seghier ML, Lazeyras F, Vuilleumier P. 2005b. View-independent coding of face identity in frontal and temporal cortices is modulated by familiarity: an event-related fMRI study. Neuroimage. 24:1214–1224.

Pourtois G, Schwartz S, Spiridon M, Martuzzi R, Vuilleumier P. 2009. Object representations for multiple visual categories overlap in lateral occipital and medial fusiform cortex. Cereb Cortex. 19(8): 1806–1819.

Puce A, Allison T, Bentin S, Gore JC, McCarthy G. 1998. Temporal cortex activation in humans viewing eye and mouth movements. J Neurosci. 18:2188–2199.

Pugliese L, Catani M, Ameis S, Dell'Acqua F, Thiebaut de Schotten M, Murphy C, Robertson D, Deeley Q, Daly E, Murphy DG. 2009. The anatomy of extended limbic pathways in Asperger syndrome: a preliminary diffusion tensor imaging tractography study. Neuroimage. 47:427–434.

Righart R, Andersson F, Schwartz S, Mayer E, Vuilleumier P. 2010. Top-down activation of fusiform cortex without seeing faces in prosopagnosia. Cereb Cortex. 20(8):1878–1890.

Rilling JK, Glasser MF, Preuss TM, Ma X, Zhao T, Hu X, Behrens TE. 2008. The evolution of the arcuate fasciculus revealed with comparative DTI. Nat Neurosci. 11:426–428.

Rossion B, Caldara R, Seghier M, Schuller AM, Lazeyras F, Mayer E. 2003. A network of occipito-temporal face-sensitive areas besides the right middle fusiform gyrus is necessary for normal face processing. Brain. 126:2381–2395.

Rotshtein P, Henson RN, Treves A, Driver J, Dolan RJ. 2005. Morphing Marilyn into Maggie dissociates physical and identity face representations in the brain. Nat Neurosci. 8:107–113.

Rotshtein P, Richardson MP, Winston JS, Kiebel SJ, Vuilleumier P, Eimer M, Driver J, Dolan RJ. 2010. Amygdala damage affects event-related potentials for fearful faces at specific time windows. Hum Brain Mapp. 31(7):1089–1105.

Rudrauf D, David O, Lachaux JP, Kovach CK, Martinerie J, Renault B, Damasio A. 2008. Rapid interactions between the ventral visual stream and emotion-related structures rely on a two-pathway architecture. J Neurosci. 28:2793–2803.

Saleem KS, Suzuki W, Tanaka K, Hashikawa T. 2000. Connections between anterior inferotemporal cortex and superior temporal sulcus regions in the macaque monkey. J Neurosci. 20:5083–5101.

Saxe R, Brett M, Kanwisher N. 2006. Divide and conquer: a defense of functional localizers. Neuroimage. 30:1088–1096; discussion 1097–1089.

Schmahmann JD, Pandya DN. 2006. Fiber pathways of the brain. Oxford: Oxford University Press.

Seltzer B, Cola MG, Gutierrez C, Massee M, Weldon C, Cusick CG. 1996. Overlapping and nonoverlapping cortical projections to cortex of the superior temporal sulcus in the rhesus monkey: double anterograde tracer studies. J Comp Neurol. 370:173–190.

Seltzer B, Pandya DN. 1978. Afferent cortical connections and architectonics of the superior temporal sulcus and surrounding cortex in the rhesus monkey. Brain Res. 149:1–24.

Seltzer B, Pandya DN. 1989. Frontal lobe connections of the superior temporal sulcus in the rhesus monkey. J Comp Neurol. 281:97–113.

Seltzer B, Pandya DN. 1994. Parietal, temporal, and occipital projections to cortex of the superior temporal sulcus in the rhesus monkey: a retrograde tracer study. J Comp Neurol. 343:445–463.

Seltzer B, Pandya DN. 2009. Posterior cingulate and retrosplenial cortex connections of the caudal superior temporal region in the rhesus monkey. Exp Brain Res. 195:325–334.

Sergent J, Ohta S, MacDonald B. 1992. Functional neuroanatomy of face and object processing. A positron emission tomography study. Brain. 115(Pt 1):15–36.

Smith SM, Jenkinson M, Johansen-Berg H, Rueckert D, Nichols TE, Mackay CE, Watkins KE, Ciccarelli O, Cader MZ, Matthews PM, et al. 2006. Tract-based spatial statistics: voxelwise analysis of multi-subject diffusion data. Neuroimage. 31:1487–1505.

Sorger B, Goebel R, Schiltz C, Rossion B. 2007. Understanding the functional neuroanatomy of acquired prosopagnosia. Neuroimage. 35:836–852.

Spiridon M, Fischl B, Kanwisher N. 2006. Location and spatial profile of category-specific regions in human extrastriate cortex. Hum Brain Mapp. 27:77–89.

Stieltjes B, Kaufmann WE, van Zijl PC, Fredericksen K, Pearlson GD, Solaiyappan M, Mori S. 2001. Diffusion tensor imaging and axonal tracking in the human brainstem. Neuroimage. 14:723–735.

Streitfeld BD. 1980. The fiber connections of the temporal lobe with emphasis on the rhesus monkey. Int J Neurosci. 11:51–71.

Thiebaut de Schotten M, Ffytche DH, Bizzi A, Dell'Acqua F, Allin M, Walshe M, Murray R, Williams SC, Murphy DG, Catani M. 2011. Atlasing location, asymmetry and inter-subject variability of white matter tracts in the human brain with MR diffusion tractography. Neuroimage. 54:49–59.

Thomas C, Avidan G, Humphreys K, Jung KJ, Gao F, Behrmann. 2009. Reduced structural connectivity in ventral visual cortex in congenital prosopagnosia. Nat Neurosci. 12(1):29–31.

Tsao DY, Moeller S, Freiwald WA. 2008. Comparing face patch systems in macaques and humans. Proc Natl Acad Sci U S A. 105:19514–19519.

Vogt BA, Pandya DN. 1987. Cingulate cortex of the rhesus monkey: II. Cortical afferents. J Comp Neurol. 262:271–289.

Vogt BA, Vogt L, Laureys S. 2006. Cytology and functionally correlated circuits of human posterior cingulate areas. Neuroimage. 29:452–466.

Vrticka P, Andersson F, Sander D, Vuilleumier P. 2009. Memory for friends or foes: the social context of past encounters with faces modulates their subsequent neural traces in the brain. Soc Neurosci. 4:384–401.

Vuilleumier P. 2005. How brains beware: neural mechanisms of emotional attention. Trends Cogn Sci. 9:585–594.

Vuilleumier P. 2007. Neural representation of faces in human visual cortex: the roles of attention, emotion, and viewpoint. In: Osaka N, Rentschler I, Biederman I, editors. Object recognition attention and action. Tokyo (Japan): Springer. p. 119–138.

Vuilleumier P, Armony JL, Driver J, Dolan RJ. 2001. Effects of attention and emotion on face processing in the human brain: an event-related fMRI study. Neuron. 30:829–841.

Vuilleumier P, Richardson MP, Armony JL, Driver J, Dolan RJ. 2004. Distant influences of amygdala lesion on visual cortical activation during emotional face processing. Nat Neurosci. 7:1271–1278.

Wahl M, Li YO, Ng J, Lahue SC, Cooper SR, Sherr EH, Mukherjee P. 2010. Microstructural correlations of white matter tracts in the human brain. Neuroimage. 51:531–541.

Wakana S, Caprihan A, Panzenboeck MM, Fallon JH, Perry M, Gollub RL, Hua K, Zhang J, Jiang H, Dubey P, et al. 2007. Reproducibility of quantitative tractography methods applied to cerebral white matter. Neuroimage. 36:630–644.

Whalen PJ, Rauch SL, Etcoff NL, McInerney SC, Lee MB, Jenike MA. 1998. Masked presentations of emotional facial expressions modulate amygdala activity without explicit knowledge. J Neurosci. 18:411–418.

Yeterian EH, Pandya DN. 1998. Corticostriatal connections of the superior temporal region in rhesus monkeys. J Comp Neurol. 399:384–402.

Zhu Q, Zhang J, Luo YL, Dilks DD, Liu J. 2011. Resting-state neural activity across face-selective cortical regions is behaviorally relevant. J Neurosci. 31:10323–10330.